*American Mineralogist, Volume 74, pages 325–332, 1989*

# Subsolidus phase equilibria near the enstatite-diopside join in $CaO$-$MgO$-$Al_2O_3$-$SiO_2$ at atmospheric pressure

WILLIAM D. CARLSON
Department of Geological Sciences, University of Texas at Austin, Austin, Texas 78713, U.S.A.

## ABSTRACT

Compositions of pyroxenes in the assemblage orthoenstatite + diopside + anorthite + forsterite have been determined by electron-microprobe analysis of experimental run products in the system $CaO$-$MgO$-$Al_2O_3$-$SiO_2$ from 925 to 1225 °C on the 1-atm isobar. The experiments, using vanadate and plumbate solvents, produced reversals of both Ca:Mg ratios and Al contents of the pyroxenes. The results confirm thermodynamic inferences that, in this assemblage, the incorporation of aluminous components in both phases is strongly dependent on pressure but largely independent of temperature, whereas the exchange of Ca and Mg between orthopyroxene and clinopyroxene is strongly dependent on temperature but largely independent of pressure. On the 1-atm isobar, the amount of Al incorporated in both pyroxenes is substantially less than present thermodynamic solution models predict.

## INTRODUCTION

Several thermodynamic analyses of the system $CaO$-$MgO$-$Al_2O_3$-$SiO_2$ (CMAS) have predicted that useful thermobarometers could be developed for feldspathic two-pyroxene mineral assemblages by quantifying the temperature dependence of the Ca-Mg exchange between orthopyroxene and clinopyroxene and the pressure dependence of the Al content of each pyroxene in equilibrium with plagioclase (e.g., Obata, 1976; Herzberg, 1978; Gasparik, 1984). The range of rock types to which such thermobarometers would be applicable is quite large, encompassing rocks as diverse as plagioclase peridotite, olivine gabbro, two-pyroxene anorthosite, and mafic granulite.

Unfortunately, these thermodynamic predictions have not yet been verified or calibrated by direct experiment. Instead, they are based upon ternary-solution models for Ca-Mg-Al pyroxenes, which are constrained by data obtained exclusively at pressures above the field of plagioclase stability. Experiments have been performed successfully only at pressures in excess of about 9 kbar, where spinel and garnet supplant feldspar as the aluminous phase in CMAS analogues to peridotitic bulk compositions (e.g., Perkins and Newton, 1980; Gasparik, 1984; Sen, 1985). The resulting thermobarometers for spinel and garnet peridotite have contributed substantially to our understanding of materials and processes in rocks of the upper mantle. However, experimental attacks on the subsolidus phase equilibria among aluminous pyroxenes at crustal temperatures and pressures (that is, in the plagioclase stability field) have so far been frustrated by extremely slow kinetics of reaction and grain growth. Conventional experimental approaches (e.g., Herzberg, 1978) typically synthesize pyroxenes too small for accurate microprobe analysis, and the sluggishness of subsolidus reaction has so far prevented the reversals of pyroxene compositions that are required to demonstrate the achievement of chemical equilibrium in such unreactive systems.

The experimental work reported here circumvented these difficulties by exploiting the kinetic advantages of the high-temperature solvent technique (Carlson, 1986a). Equilibrium compositions of coexisting, anorthite-saturated orthopyroxene and clinopyroxene, constrained by reversals of both Ca:Mg ratios and alumina contents, have been determined at 50 °C increments from 925 to 1225 °C on the 1-atm isobar. The results provide a low-pressure benchmark for higher-pressure experimentation and for the thermodynamic analysis of equilibria pertinent to feldspathic two-pyroxene assemblages in a variety of crustal rocks.

## EXPERIMENTAL PROCEDURES AND EQUILIBRIUM CRITERIA

The experimental and analytical procedures employed in this study were nearly identical to those in earlier work in the CMS system (Carlson, 1988). Most experiments were performed with vanadate solvents as described in Carlson (1986a), but a few confirmatory syntheses employed plumbate solvents for comparison; all solvent compositions are shown in Figure 1. In all experiments, the proportion by weight of solvent to other reactants was in the range of 1:1 to 4:1. Reactants were loaded in 3-cm-long, 2.5-mm-diameter Pt capsules and dried at 600 °C for 48 h before the capsules were sealed. Charges were held in a vertical quench furnace for periods of 3 to 7 d at the desired temperature, measured by $Pt$-$Pt_{90}Rh_{10}$ thermocouples with an accuracy estimated at ±5 °C on the basis of repeated calibrations against the melting point of

0003–004X/89/0304–0325$02.00

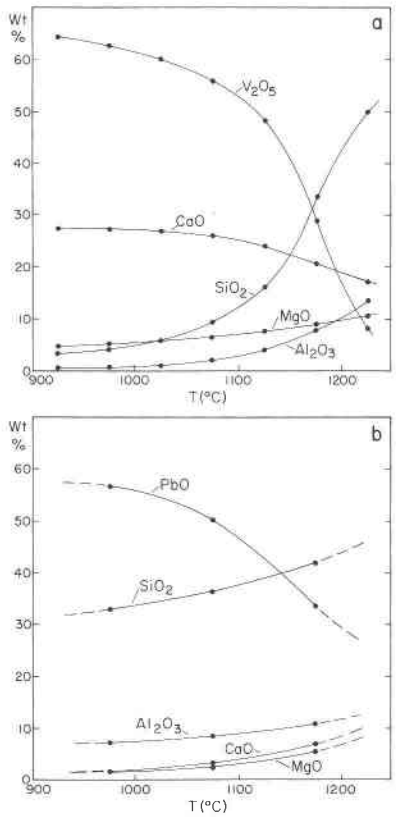


Fig. 1. Compositions of (**a**) vanadate solvents and (**b**) plumbate solvents saturated with respect to En + Di + An + Fo, as determined by electron-microprobe analysis of quenched melts.

Au and the liquidus of $CaMgSi_2O_6$. Runs were quenched into water, then dried at 110 °C before small chips were removed and polished for examination in reflected light and for microprobe analysis. The remainder of the charge was leached of solvent using 4% HCl for vanadates and hot 1:1 $HNO_3$ for plumbates, then boiled for 2 to 3 min in 0.5*M* NaOH to dissolve small amounts of residual silica-rich gel. The crystalline run products extracted in this way were examined petrographically in immersion media and analyzed by X-ray powder diffraction. Microprobe analysis on a JEOL 733 instrument employed wavelength-dispersive techniques with 60-s counting times for a sample current of 15 nA on brass at an accelerating potential of 15 kV. Analytical standards were a synthetic glass containing CaO, MgO, $Al_2O_3$, FeO, and $SiO_2$ (NBS Standard Reference Material #470 = Glass K412) for Ca, Mg, Al, and Si; synthetic crystalline $V_2O_5$ for V; and a synthetic lead silicate glass (NBS Standard Reference Material #1871 = Glass K456) for Pb.

To demonstrate the attainment of equilibrium partitioning of Ca, Mg, and Al between coexisting pyroxenes, four types of reactant materials were required. These reactants (designated A, B, C, and D in Table 1) have identical bulk chemistry but different mineral compositions. In contrast to the previous study in CMS (Carlson, 1988), synthesis of crystalline reactant materials directly from glass at 1 atm was not feasible; such attempts typically produced variable amounts of aluminous protoenstatite (Pen), in addition to the desired starting assemblage consisting of solid solutions of orthoenstatite + diopside + anorthite + forsterite (En + Di + An + Fo). Consequently, reactant mixes were produced in a multistage procedure. Reagent oxides in amounts that would yield equimolar proportions of $Mg_2Si_2O_6$, $CaMgSi_2O_6$, $CaAl_2Si_2O_8$, and $Mg_2SiO_4$ were first ground and fused through several cycles, then were crystallized hydrothermally for 14 d at 850 °C and 1 kbar $H_2O$ to yield a very finely crystalline mixture of En + Di + An + Fo. This material was then recrystallized in the presence of vanadate solvents at 925 °C and 1 atm, at 1225 °C and 1 atm, and (in an internally heated pressure vessel) at 1025 °C and 5 kbar, to produce reactants A, B, and C respectively. Reactant D consisted of a mixture of (1) anorthite crystallized hydrothermally from oxides at 850 °C and 2 kbar $H_2O$ for 28 d and (2) an Al-free assemblage of En + Di + Fo crystallized hydrothermally from glass at 850 °C and 2 kbar $H_2O$ for 14 d; these were mixed in proportions to yield a composition identical to that of the other three reactants.

**Table 1.** Compositions of pyroxenes in reactants

| Reactant | Synthesis conditions | Orthoenstatite Ca/(Ca + Mg) | Orthoenstatite $X_{mt}$ | Diopside Ca/(Ca + Mg) | Diopside $X_{ct}$ |
|---|---|---|---|---|---|
| A* | 925 °C, 1 bar | 0.033 | 0.016 | 0.458 | 0.016 |
| B* | 1225 °C, 1 bar | 0.049 | 0.023 | 0.395 | 0.029 |
| C* | 1075 °C, 5 kbar | 0.023 | 0.047 | 0.473 | 0.043 |
| D† | 850 °C, 2 kbar | 0.006 | 0 | 0.465 | 0 |

* Compositions determined by electron-microprobe analysis.
† Too small for microprobe analysis; Ca/(Ca + Mg) assumed to be equilibrium value calculated from thermodynamic model of Carlson and Lindsley (1988).

Because CMAS pyroxenes are ternary solutions, it is not a straightforward procedure to demonstrate convincingly the reversal of phase compositions (cf. Gasparik, 1984, p. 87; Sen, 1985, p. 679). Fortunately, thermodynamic analysis and reconnaissance synthesis experiments in this system suggest that in the field of plagioclase stability, Ca:Mg ratios in the pyroxenes are largely independent of pressure, whereas the incorporation of Al into the pyroxenes is largely independent of temperature. Thus reactants A and B (which have closely similar Al contents, but which have bounding values for Ca:Mg ratios at 1 atm) should react toward equilibrium in such a way as to bracket the equilibrium Ca:Mg ratios. Reactants C and D (which have bounding values of Al content, despite differences in Ca:Mg ratios) should react toward equilibrium in such a way as to bracket the equilibrium Al content. The combination of these two complementary sets of reversals therefore tightly constrains the ternary compositions at equilibrium. In fact, the data below confirm that, especially at high temperatures, all four

**TABLE 2.** Averages of diopside compositions in reversals using $V_2O_5$ solvents

| Temp (°C) | Reactant | n | Weight percent | | | | | | Cations per 6 oxygens | | Mole fraction | | | Molar Ca |
|---|---|---|---|---|---|---|---|---|---|---|---|---|---|---|
| | | | CaO | MgO | $Al_2O_3$ | $SiO_2$ | $V_2O_3$ | Total | [6] | [4] | di | en | ct | (Ca + Mg) |
| 925 | B | 37 | 23.44 | 20.55 | 0.85 | 55.33 | 0.34 | 100.51 | 2.01 | 1.99 | 0.877 | 0.105 | 0.018 | 0.451 |
| | C | 10 | 23.71 | 19.90 | 0.97 | 55.07 | 0.61 | 100.26 | 2.00 | 1.99 | 0.888 | 0.092 | 0.020 | 0.461 |
| | D | 10 | 23.45 | 20.27 | 0.63 | 55.24 | 0.73 | 100.32 | 2.01 | 1.99 | 0.884 | 0.103 | 0.013 | 0.454 |
| 975 | A | 8 | 23.45 | 20.35 | 0.71 | 55.04 | 0.56 | 100.11 | 2.01 | 1.99 | 0.884 | 0.101 | 0.015 | 0.453 |
| | B | 15 | 23.19 | 20.49 | 0.73 | 55.17 | 0.48 | 100.06 | 2.01 | 1.99 | 0.874 | 0.111 | 0.015 | 0.449 |
| | C | 10 | 23.42 | 20.07 | 1.09 | 55.13 | 0.63 | 100.34 | 2.00 | 1.99 | 0.873 | 0.104 | 0.023 | 0.456 |
| | D | 14 | 23.00 | 20.53 | 0.71 | 54.41 | 0.65 | 99.30 | 2.03 | 1.98 | 0.874 | 0.111 | 0.015 | 0.446 |
| 1025 | A | 8 | 23.38 | 20.62 | 0.85 | 55.24 | 0.57 | 100.66 | 2.02 | 1.98 | 0.874 | 0.108 | 0.018 | 0.449 |
| | B | 17 | 22.91 | 20.78 | 0.78 | 55.04 | 0.41 | 99.92 | 2.01 | 1.99 | 0.862 | 0.121 | 0.017 | 0.442 |
| | C | 9 | 22.95 | 20.56 | 1.10 | 55.21 | 0.65 | 100.47 | 2.01 | 1.99 | 0.853 | 0.129 | 0.018 | 0.443 |
| | D | 7 | 22.91 | 20.74 | 0.85 | 55.57 | 0.67 | 100.74 | 2.00 | 1.99 | 0.853 | 0.129 | 0.018 | 0.443 |
| 1075 | A | 9 | 22.79 | 21.14 | 0.71 | 55.18 | 0.41 | 100.23 | 2.02 | 1.98 | 0.857 | 0.129 | 0.015 | 0.437 |
| | B | 8 | 22.71 | 21.28 | 0.91 | 55.10 | 0.34 | 100.34 | 2.03 | 1.98 | 0.848 | 0.133 | 0.019 | 0.434 |
| | C | 11 | 22.20 | 20.99 | 1.15 | 54.98 | 0.68 | 100.00 | 2.01 | 1.99 | 0.825 | 0.151 | 0.024 | 0.432 |
| | D | 8 | 22.03 | 21.20 | 0.94 | 55.55 | 0.69 | 100.41 | 2.00 | 1.99 | 0.818 | 0.162 | 0.020 | 0.428 |
| 1125 | A | 10 | 22.13 | 21.40 | 0.77 | 54.96 | 0.61 | 99.87 | 2.02 | 1.98 | 0.832 | 0.152 | 0.016 | 0.426 |
| | B | 14 | 21.80 | 21.38 | 1.28 | 55.10 | 0.56 | 100.12 | 2.01 | 1.99 | 0.805 | 0.168 | 0.027 | 0.423 |
| | C | 13 | 21.70 | 21.34 | 1.17 | 55.04 | 0.60 | 99.85 | 2.01 | 1.99 | 0.806 | 0.170 | 0.025 | 0.422 |
| | D | 5 | 21.89 | 21.23 | 1.07 | 54.87 | 0.63 | 99.69 | 2.01 | 1.99 | 0.817 | 0.161 | 0.023 | 0.426 |
| 1175 | A | 10 | 21.88 | 21.50 | 0.96 | 55.22 | 0.48 | 100.04 | 2.01 | 1.99 | 0.816 | 0.164 | 0.020 | 0.423 |
| | B | 11 | 20.30 | 22.03 | 1.36 | 55.23 | 0.46 | 99.38 | 1.99 | 2.00 | 0.748 | 0.224 | 0.029 | 0.399 |
| | C | 13 | 20.75 | 21.98 | 1.27 | 55.54 | 0.49 | 100.03 | 1.99 | 2.00 | 0.762 | 0.211 | 0.027 | 0.404 |
| | D | 12 | 21.50 | 21.55 | 1.27 | 55.25 | 0.46 | 100.03 | 2.00 | 1.99 | 0.793 | 0.180 | 0.027 | 0.418 |
| 1225 | A | 15 | 20.75 | 22.12 | 1.25 | 55.39 | 0.27 | 99.78 | 2.00 | 2.00 | 0.765 | 0.209 | 0.026 | 0.403 |
| | C | 15 | 20.25 | 22.53 | 1.45 | 55.84 | 0.32 | 100.39 | 1.99 | 2.00 | 0.735 | 0.234 | 0.030 | 0.393 |
| | D | 15 | 20.57 | 22.50 | 1.42 | 55.92 | 0.26 | 100.67 | 1.99 | 2.00 | 0.747 | 0.223 | 0.030 | 0.397 |

*Note:* $n$ = number of crystals analyzed; [6] = Ca + Mg + Al/2 + V; [4] = Si + Al/2; ct = Al/2; di = Ca − Al/2; en = 1 − ct − di.

reactants converged upon nearly identical pyroxene compositions.

## EXPERIMENTAL RESULTS

All experiments for which pyroxene compositions are reported produced the assemblage En + Di + An + Fo. In these runs, orthoenstatite and diopside crystallize as stubby 5- to 20-$\mu$m-long prisms, forsterite appears as subequant to slightly elongate euhedra of comparable size to the pyroxenes, but anorthite is typically found as markedly smaller (1–5 $\mu$m) individual laths or in rounded aggregates of still smaller crystals. All phases appearing in runs using plumbate solvents are colorless, but in runs using vanadate solvents, small amounts of V in the pyroxenes cause them to be slightly colored. In powdered aggregates, orthoenstatite is faintly yellow-green; it displays weak pleochroism from yellow-green to colorless when examined petrographically. Diopside is very pale blue in powdered aggregates, but the coloration is too faint to be seen in light transmitted through individual crystals. Anorthite and forsterite in these runs are uncolored.

Tables 2 and 3 present the compositions of diopside and orthoenstatite in runs using vanadate solvents, as determined by electron-microprobe analysis; Table 4 presents pyroxene compositions in synthesis experiments using plumbate solvents. Diopside is regarded as a solid solution of the components $Mg_2Si_2O_6$, $CaMgSi_2O_6$, and $CaAl_2SiO_6$, which are designated by the two-letter lower-case abbreviations en, di, and ct (for Ca-Tschermak's component); mole fractions ($X$) are defined, using numbers of cations per six oxygens, by $X_{ct}^{Di} \equiv Al/2$; $X_{di}^{Di} \equiv Ca - Al/2$; $X_{en}^{Di} \equiv 1 - Ca$. Orthoenstatite is regarded as a solid solution of the components $Mg_2Si_2O_6$, $CaMgSi_2O_6$, and $MgAl_2SiO_6$, which are designated by the two-letter lower-case abbreviations en, di, and mt (for Mg-Tschermak's component); mole fractions ($X$) are defined, using numbers of cations per six oxygens, by $X_{mt}^{En} \equiv Al/2$; $X_{di}^{En} \equiv Ca$; $X_{en}^{En} \equiv 1 - Ca - Al/2$. The use of Tschermak's components implicitly allocates Al equally between octahedral and tetrahedral sites. The total site occupancies listed in Tables 2 and 3 are consistent with this scheme of allocation. To estimate analytical uncertainties for the quantities important to thermobarometric applications, standard errors of the mean for each oxide in the microprobe analyses were propagated through the calculation of Ca/(Ca + Mg) ratios and mole fractions of components. In diopside, analytical uncertainties in Ca/(Ca + Mg) range from about 0.0010 to 0.0020, and average 0.0015; analytical uncertainties in $X_{ct}$ range from about 0.0001 to 0.0008, although most are near the average of 0.0003. In orthoenstatite, analytical uncertainties in Ca/(Ca + Mg) are all less than 0.0010; analytical uncertainties in $X_{mt}$ range from about 0.0002 to 0.0005, with an average of 0.0003.

Figure 2 depicts the CMAS phase relations between

**TABLE 3.** Averages of orthoenstatite compositions in reversals using $V_2O_5$ solvents

| Temp (°C) | Reactant | n | Weight percent | | | | | | Cations per 6 oxygens | | Mole fraction | | | Molar Ca |
|---|---|---|---|---|---|---|---|---|---|---|---|---|---|---|
| | | | CaO | MgO | $Al_2O_3$ | $SiO_2$ | $V_2O_3$ | Total | [6] | [4] | di | en | mt | (Ca + Mg) |
| 925 | B | 21 | 2.32 | 38.39 | 0.94 | 58.63 | 0.26 | 100.54 | 2.03 | 1.98 | 0.083 | 0.917 | 0.019 | 0.042 |
| | C | 3 | 1.69 | 37.67 | 1.16 | 58.40 | 0.70 | 99.62 | 2.00 | 1.99 | 0.061 | 0.939 | 0.023 | 0.031 |
| | D | 7 | 1.81 | 37.79 | 0.78 | 59.24 | 0.60 | 100.22 | 1.98 | 2.00 | 0.065 | 0.935 | 0.015 | 0.033 |
| 975 | A | 16 | 2.14 | 38.05 | 0.82 | 58.60 | 0.45 | 100.06 | 2.01 | 1.99 | 0.077 | 0.923 | 0.016 | 0.039 |
| | B | 38 | 2.22 | 38.01 | 0.89 | 58.61 | 0.30 | 100.03 | 2.01 | 1.99 | 0.080 | 0.920 | 0.018 | 0.040 |
| | C | 4 | 1.69 | 37.85 | 1.05 | 57.94 | 0.59 | 99.12 | 2.01 | 1.99 | 0.066 | 0.934 | 0.016 | 0.033 |
| | D | 14 | 1.82 | 38.02 | 0.80 | 58.64 | 0.72 | 100.00 | 2.01 | 1.99 | 0.066 | 0.934 | 0.016 | 0.033 |
| 1025 | A | 20 | 2.10 | 37.94 | 0.84 | 58.84 | 0.40 | 100.12 | 2.00 | 1.99 | 0.076 | 0.924 | 0.017 | 0.038 |
| | B | 35 | 2.26 | 37.93 | 0.88 | 59.02 | 0.29 | 100.38 | 2.00 | 2.00 | 0.081 | 0.919 | 0.017 | 0.041 |
| | C | 6 | 2.02 | 37.87 | 1.08 | 59.07 | 0.56 | 100.60 | 1.99 | 2.00 | 0.072 | 0.928 | 0.021 | 0.037 |
| | D | 9 | 2.11 | 37.87 | 0.93 | 58.84 | 0.56 | 100.31 | 2.00 | 1.99 | 0.076 | 0.924 | 0.019 | 0.038 |
| 1075 | A | 8 | 2.25 | 38.04 | 1.14 | 58.76 | 0.45 | 100.64 | 2.01 | 1.99 | 0.081 | 0.920 | 0.023 | 0.041 |
| | B | 30 | 2.27 | 37.94 | 0.85 | 58.78 | 0.34 | 100.18 | 2.01 | 1.99 | 0.082 | 0.918 | 0.017 | 0.041 |
| | C | 5 | 2.24 | 37.85 | 1.06 | 58.53 | 0.49 | 100.17 | 2.01 | 1.99 | 0.081 | 0.919 | 0.021 | 0.041 |
| | D | 5 | 2.25 | 37.90 | 1.04 | 58.61 | 0.54 | 100.34 | 2.01 | 1.99 | 0.081 | 0.919 | 0.021 | 0.041 |
| 1125 | A | 11 | 1.96 | 38.13 | 0.68 | 59.09 | 0.41 | 100.27 | 2.00 | 1.99 | 0.071 | 0.930 | 0.013 | 0.036 |
| | B | 15 | 2.52 | 37.62 | 1.23 | 58.71 | 0.41 | 100.49 | 2.00 | 1.99 | 0.090 | 0.910 | 0.024 | 0.046 |
| | C | 15 | 2.22 | 37.64 | 1.09 | 58.44 | 0.48 | 99.87 | 2.00 | 1.99 | 0.080 | 0.920 | 0.022 | 0.041 |
| | D | 10 | 2.40 | 38.02 | 1.03 | 58.99 | 0.47 | 100.91 | 2.01 | 1.99 | 0.086 | 0.914 | 0.020 | 0.043 |
| 1175 | A | 15 | 2.41 | 37.75 | 0.85 | 58.96 | 0.38 | 100.35 | 2.00 | 1.99 | 0.087 | 0.913 | 0.017 | 0.044 |
| | B | 15 | 2.57 | 37.55 | 1.22 | 58.81 | 0.29 | 100.44 | 2.00 | 2.00 | 0.092 | 0.908 | 0.024 | 0.047 |
| | C | 13 | 2.41 | 37.77 | 1.09 | 58.67 | 0.32 | 100.26 | 2.01 | 1.99 | 0.087 | 0.913 | 0.022 | 0.044 |
| | D | 11 | 2.53 | 37.21 | 0.88 | 58.67 | 0.37 | 99.66 | 1.99 | 2.00 | 0.092 | 0.908 | 0.018 | 0.047 |
| 1225 | A | 13 | 2.69 | 37.23 | 1.08 | 58.57 | 0.13 | 99.70 | 2.00 | 2.00 | 0.098 | 0.903 | 0.022 | 0.049 |
| | C | 14 | 2.73 | 37.60 | 1.26 | 59.12 | 0.14 | 100.85 | 2.00 | 2.00 | 0.098 | 0.902 | 0.025 | 0.050 |
| | D | 14 | 2.70 | 37.53 | 1.25 | 59.04 | 0.09 | 100.61 | 2.00 | 2.00 | 0.097 | 0.903 | 0.025 | 0.049 |

*Note:* n = number of crystals analyzed; [6] = Ca + Mg + Al/2 + V; [4] = Si + Al/2; mt = Al/2; di = Ca; en = 1 − mt − di.

coexisting orthopyroxene and clinopyroxene, in equilibrium with anorthite and forsterite, at 1-atm pressure, from 925 °C to the solidus at 1240 °C. The reversals shown by the arrowheads are based only upon runs using reactants A and B, which have closely similar Al contents, but ratios of Ca:Mg that cause the run products to approach the equilibrium compositions from both higher and lower values of Ca/(Ca + Mg). Those brackets are in excellent agreement with the compositions in Tables 2 and 3 for pyroxenes in runs using the other reactants as well.

Figure 3 illustrates the slight temperature dependence at atmospheric pressure of the aluminous components in coexisting orthopyroxene and clinopyroxene, both saturated with respect to anorthite and forsterite. The reversals shown by the arrowheads are based only upon runs using reactants C and D, which have slightly different ratios of Ca:Mg, but which approach the equilibrium Al content from markedly higher and lower values, respectively. Once again, the data on Al contents in Tables 2 and 3, from runs using the other two reactants, are in excellent agreement with the relationships portrayed in Figure 3.

Figure 4 summarizes, on a pair of ternary diagrams, the changes in pyroxene compositions with temperature at atmospheric pressure in the assemblage En + Di + An + Fo. Data points plotted for each temperature were obtained from the lines connecting the brackets in Figures 2 and 3, and therefore represent graphical interpolations from the actual analyses.

Table 5 presents representative analyses of anorthite

**TABLE 4.** Averages of diopside and orthoenstatite compositions in syntheses using PbO solvents

| Temp (°C) | Phase | n | Weight percent | | | | | | Cations per 6 oxygens | | Mole fraction | | | Molar Ca |
|---|---|---|---|---|---|---|---|---|---|---|---|---|---|---|
| | | | CaO | MgO | $Al_2O_3$ | $SiO_2$ | PbO | Total | [6] | [4] | di | en | ct/mt | (Ca + Mg) |
| 975 | Di | 6 | 22.94 | 20.66 | 0.87 | 56.17 | n.d. | 100.65 | 1.98 | 2.01 | 0.853 | 0.129 | 0.018 | 0.444 |
| | En | 10 | 1.99 | 37.90 | 0.93 | 58.94 | n.d. | 99.76 | 1.99 | 2.00 | 0.072 | 0.909 | 0.019 | 0.036 |
| 1075 | Di | 13 | 22.42 | 20.57 | 0.98 | 55.50 | n.d. | 99.46 | 1.98 | 2.01 | 0.840 | 0.144 | 0.021 | 0.437 |
| | En | 11 | 2.28 | 37.58 | 1.07 | 58.93 | n.d. | 99.86 | 1.99 | 2.01 | 0.082 | 0.897 | 0.021 | 0.042 |
| 1175 | Di | 5 | 20.87 | 22.23 | 0.86 | 55.31 | n.d. | 99.26 | 2.00 | 2.00 | 0.782 | 0.200 | 0.018 | 0.403 |
| | En | 5 | 2.30 | 37.67 | 1.11 | 58.24 | n.d. | 99.32 | 2.01 | 2.00 | 0.084 | 0.894 | 0.022 | 0.042 |

*Note:* n = number of crystals analyzed; n.d. = below detection limit of ~0.01; [6] = Ca + Mg + Al/2; [4] = Si + Al/2; di, en, and ct computed for Di as in Table 2; di, en, and mt computed for En as in Table 3.

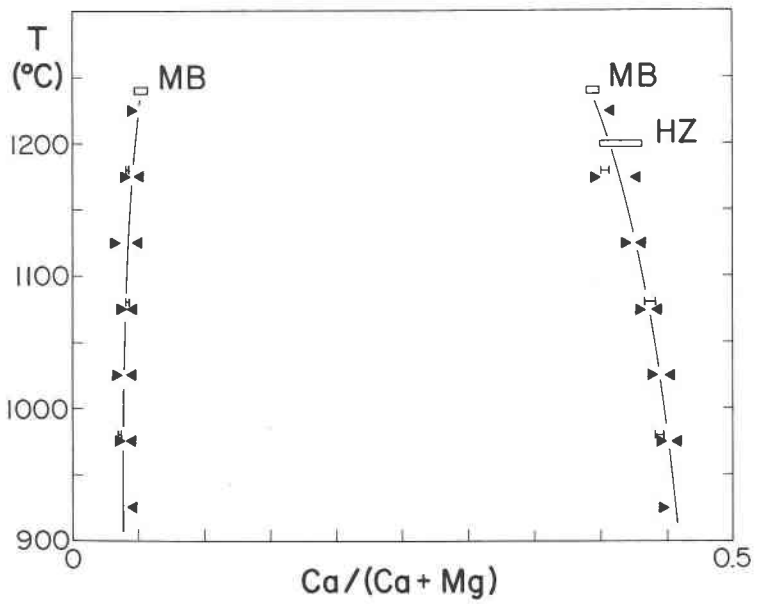


Fig. 2. The ratio Ca/(Ca + Mg) in coexisting orthoenstatite and diopside, both simultaneously in equilibrium with anorthite and forsterite, as a function of temperature at 1-atm pressure. The compositions of pyroxenes from reversal runs, using vanadate solvents with reactants A and B, are plotted as arrowheads indicating the direction of approach to equilibrium, with the arrowpoint located at the mean composition in the run. The compositions of confirmatory synthesis runs in plumbate solvents are plotted as error bars centered on the mean composition of the run, with widths equal to twice the standard error of the mean of the analyzed compositions. Synthesis results of Mori and Biggar (1981) ["MB," on the solidus] and of Herzberg (1978) ["HZ," subsolidus] are shown by rectangles centered on the mean analyzed composition, with widths equal to twice the published estimates of error. Lines defining the miscibility gap were drawn by eye to fit the data as smoothly as possible.

crystals from runs using both vanadate and plumbate solvents. The low mole fractions of V and Pb components signify that the activity of $CaAl_2Si_2O_8$ in plagioclase in these experimental runs is likely to be near unity. The following discussion sets forth additional evidence that the small amounts of solvent components in both plagioclase and pyroxene have only negligible effects upon the equilibria under study.

## Discussion

### Comparison with previous studies

Because of the experimental difficulties cited above, few analyses are available in the literature that afford a direct comparison with the data presented here. Perhaps the most reliable data are those of Mori and Biggar (1981) for the compositions of coexisting pyroxenes in silicate melts at temperatures very near the solidus for this assemblage at 1240 °C. [Although the low-Ca pyroxene in their runs was originally identified as protoenstatite in their Table 27, it has subsequently been recognized as orthoenstatite (Biggar, 1985, p. 54).] The data of Mori and Biggar, obtained by electron-microprobe analysis, are shown by the rectangles labeled "MB" in Figures 2 and 3. They compare very favorably with the results of this study.

In the subsolidus region, only one measurement of the composition of diopside in equilibrium with orthoensta-

**Table 5.** Averages of anorthite compositions

| Temp (°C) | n | Weight percent | | | | | | Cations per 8 oxygens | | | | | Mole fraction $CaAl_2Si_2O_8$ |
|---|---|---|---|---|---|---|---|---|---|---|---|---|---|
| | | CaO | $Al_2O_3$ | $SiO_2$ | $V_2O_3$ | PbO | Total | Ca | Al | Si | V | Pb | |
| 975 | 15 | 19.90 | 36.29 | 43.03 | 0.21 | n.p. | 99.43 | 0.992 | 1.993 | 2.003 | 0.008 | n.p. | 0.996 |
| | 13 | 20.35 | 36.47 | 43.66 | n.p. | 0.40 | 100.88 | 1.004 | 1.981 | 2.010 | n.p. | 0.005 | 0.995 |
| 1075 | 13 | 20.11 | 36.44 | 43.21 | 0.22 | n.p. | 99.98 | 0.998 | 1.992 | 2.001 | 0.008 | n.p. | 0.996 |
| | 14 | 19.97 | 36.52 | 42.89 | n.p. | 0.42 | 99.80 | 0.996 | 2.005 | 1.996 | n.p. | 0.005 | 0.995 |
| 1175 | 15 | 20.08 | 37.02 | 43.49 | 0.22 | n.p. | 100.81 | 0.988 | 2.005 | 1.996 | 0.008 | n.p. | 0.996 |
| | 15 | 20.02 | 36.39 | 43.58 | n.p. | 0.36 | 100.35 | 0.991 | 1.984 | 2.014 | n.p. | 0.004 | 0.996 |

*Note:* $n$ = number of crystals analyzed; n.p. = not present; mole fractions computed as Al/(Al + V) and as Ca/(Ca + Pb), i.e., assuming substitution of V for Al and of Pb for Ca.

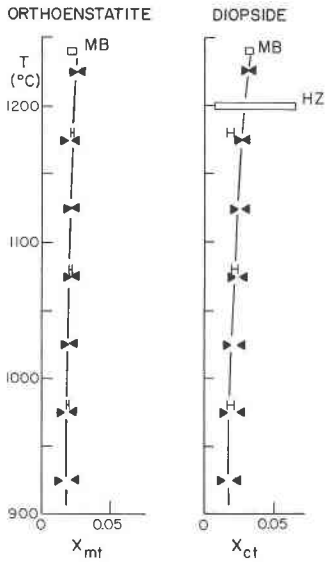


Fig. 3. Mole fraction of aluminous components in orthoenstatite and diopside saturated with respect to plagioclase, simultaneously in equilibrium with one another and with forsterite, as a function of temperature at 1-atm pressure. The compositions of pyroxenes from reversal runs, using vanadate solvents with reactants C and D, are plotted as arrowheads indicating the direction of approach to equilibrium, with the arrowpoint located at the mean composition in the run. The compositions of confirmatory synthesis runs in plumbate solvents are plotted as error bars centered on the mean composition of the run, with widths equal to twice the standard error of the mean of the analyzed compositions. Synthesis results of Mori and Biggar (1981) ["MB," on the solidus] and of Herzberg (1978) ["HZ," subsolidus] are shown by rectangles centered on the mean analyzed composition, with widths equal to twice the published estimates of error. Lines between brackets were drawn by eye to fit the data as smoothly as possible.

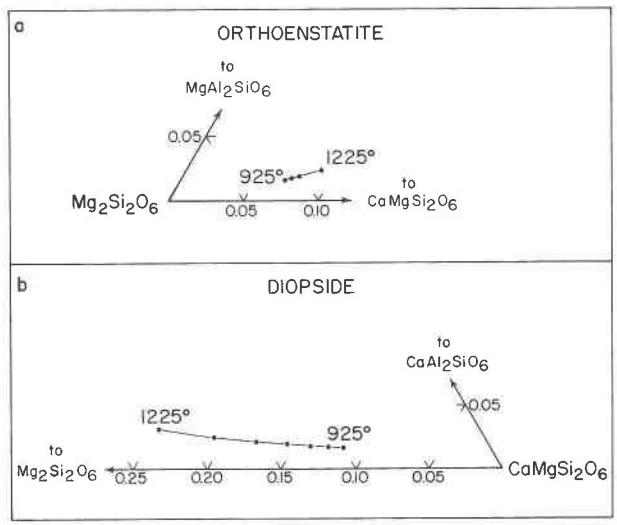


Fig. 4. Ternary diagrams illustrating the changes in compositions of coexisting orthoenstatite and diopside (saturated with respect to anorthite and forsterite) as a function of temperature at atmospheric pressure. Plotted points are taken from fitted lines appearing in Figures 2 and 3. (**a**) Orthoenstatite compositions in 100 °C increments from 925 to 1225 °C. (**b**) Diopside compositions in 50 °C increments from 925 to 1225 °C.

tite, forsterite, and anorthite at atmospheric pressure is available. Herzberg (1978, Table A1) presents a synthesis result at 1200 °C for which the composition of diopside was estimated from determinative curves based upon lattice spacings obtained by X-ray powder diffraction. Despite the relatively large uncertainties that characterize this datum, its position in Figures 2 and 3 (as the rectangle labeled "HZ") is in good agreement with the present subsolidus results. If Herzberg's datum were to be adjusted in accordance with revised determinative curves published by Benna et al. (1981), the agreement with the present data would be slightly better.

Finally, the compositions of orthoenstatite resulting from this study may be compared to the compilation of data on low-Ca pyroxenes that appears as Figure 6 of Biggar (1985). Appropriately for pyroxene saturated with respect to plagioclase and diopside, the orthoenstatite compositions from this study plot near the high-Al, high-Ca apex of Biggar's orthoenstatite field. They lie in close proximity to several somewhat scattered microprobe analyses made by Mori (as cited in Biggar, 1985, caption to his Fig. 6) for orthoenstatite coexisting with anorthite and diopside.

## Effects of solvents on phase equilibria

Whenever the high-temperature solvent technique is applied, it is essential to assess the effects of any small amounts of the solvent components incorporated into the phases of interest. Experience gained in a study of CMS pyroxenes, using similar vanadate and plumbate solvents, indicates that the effects of these solvents on the pyroxene phase equilibria are negligible (Carlson, 1988, p. 240). That conclusion is corroborated in this study by the correspondence noted above between pyroxene compositions arising from conventional experiments and those obtained in this work. In particular, the agreement upon the Al content of pyroxenes between this study and the data of Mori and Biggar (1981) can be regarded as evidence that the activity of $CaAl_2Si_2O_8$ in plagioclase is not significantly below unity in the experiments reported here. Furthermore, because the vanadate and plumbate solvents are expected to produce opposite crystallochemical effects in the pyroxenes (as a result of the contrast between the ionic radii of V and Pb), it is encouraging that the synthesis experiments in plumbate solvents agree well with the reversed equilibria determined in vanadate solvents. The close coincidence of the pyroxene compositions from runs using different solvents indicates that neither solvent has an appreciable effect upon the equilibria under study.

As in the previous study in CMS (Carlson, 1988, p. 240), the fact that analyzed V contents in the pyroxenes tend to decrease and show less scatter at higher temper-

atures probably signifies that much of the V in the pyroxenes may reside not within the crystal lattice, but in tiny inclusions of quenched melt, which are more numerous in crystals produced at lower temperatures. Consequently, it is likely that the analyses overestimate the amounts of V actually present in solid solution within the pyroxenes.

In earlier work using vanadate solvents (Carlson, 1986b, p. 222), V in CMS pyroxenes was inferred to be in the tetravalent state, substituting for Si in tetrahedral sites. Subsequently, however, reflectance spectra of Al-free CMS run products have revealed only $V^{3+}$ in octahedral coordination: in Figure 5, the bands near 0.6 and 1.1 $\mu$m have energies similar to those of octahedral $V^{3+}$ in corundum and the aqueous $V^{3+}$ ion (cf. Marfunin, 1979, p. 208). Insofar as no other species in the CMS system can provide charge balance for octahedral $V^{3+}$, substitution of two $V^{3+}$ and an octahedral vacancy for three divalent cations in octahedral sites is implied. Al-bearing CMAS pyroxenes are colored identically to CMS pyroxenes, so that a similar mode of incorporation of $V^{3+}$ can reasonably be inferred for the run products in this work.

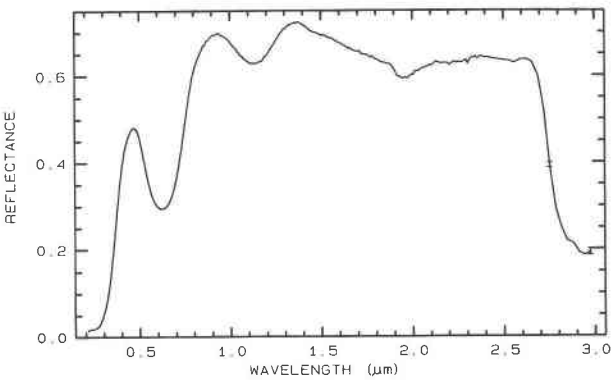


Fig. 5. Reflectance spectrum of Al-free (CMS) diopside from runs using vanadate solvents, confirming the presence of vanadium as $V^{3+}$ in octahedral coordination. The spectrum of Al-free (CMS) orthoenstatite is nearly identical. Spectroscopic data were obtained and interpreted by D. Sherman of the U.S. Geological Survey.

### Pen + En equilibria

Several synthesis runs, made in reconnaissance for the purpose of determining solvent compositions, were sufficiently undersaturated in CaO to produce the assemblage Pen + En + Fo + An. Microprobe analysis of the pyroxenes indicates that, from 1025 to 1225 °C, (1) the ratio Ca/(Ca + Mg) in protoenstatite increases from about 0.012 to 0.014, while the same ratio in orthoenstatite increases from about 0.037 to 0.048; and (2) both $X_{mt}^{Pen}$ and $X_{mt}^{En}$ increase from about 0.018 to 0.025. Orthoenstatite in this assemblage therefore appears to have compositions closely similar to those of orthoenstatite equilibrated with diopside, suggesting that the one-phase field for orthoenstatite at atmospheric pressure is restricted by very narrow limits in this system. No attempt was made, however, to verify these relationships by experimental reversals of pyroxene compositions.

## Implications and conclusions

The data of Figures 2, 3, and 4 confirm the thermodynamic predictions that useful pyroxene thermometers and barometers can be developed for feldspathic rocks once proper experimental calibration is complete. In particular, the very slight temperature dependence of $X_{ct}^{Di}$ and $X_{mt}^{En}$ on the 1-atm isobar (Fig. 3) indicates that these quantities should serve as excellent petrologic barometers, considering the marked increase in Al content with pressure suggested by the 5-kbar synthesis reported here and the synthesis results of Herzberg (1978, Table A1) at 3.2, 5.0, and 7.0 kbar.

It is not surprising to find some discrepancies between these experimental results and the predictions (at atmospheric pressure) of the most recent thermodynamic model for CMAS phase relations in the plagioclase stability field (Gasparik, 1984). In fact, considering the complete absence of low-pressure data to constrain the model, it is remarkable that the discrepancies are as small as they are. Thermometric agreement is excellent: experimental values of $X_{en}^{Di}$ range from 0.098 at 925 °C to 0.216 at 1225 °C, compared to model values of 0.097 to 0.240 for the same range of temperature. Barometric predictions of the model are low by several kilobars. Gasparik's model overestimates the amounts of Al in each pyroxene: from 925 to 1225 °C, measured $X_{mt}^{En}$ ranges from 0.017 to 0.025, compared to model values of 0.032 to 0.043, and measured $X_{ct}^{Di}$ ranges from 0.017 to 0.031, compared to model values of 0.028 to 0.044.

Further experimentation at elevated pressures within the plagioclase stability field will certainly be required to properly calibrate such models. Nevertheless, this study provides a benchmark at atmospheric pressure that will constrain, and yet should encourage, experimental efforts at higher pressure. It is a first step toward the development of well-constrained thermobarometers applicable to a wide variety of feldspathic mafic and ultramafic rocks in the Earth's crust.

## Acknowledgments

Support for this work was provided by NSF grant EAR-8603755 to the author, by the University of Texas Research Institute, and by the Geology Foundation of the University of Texas at Austin. The synthesis of reactant C was carried out in an internally heated pressure vessel in the Experimental Petrology Laboratory at NASA's Johnson Space Center, Houston, Texas. I am especially grateful to G. Lofgren for making that work possible, and I thank W. Carter for technical assistance in those experiments. Special thanks are extended to D. Sherman of the U.S. Geological Survey, Denver, Colorado, who kindly measured and interpreted reflectance spectra on samples of vanadian pyroxenes. D. Perkins contributed a helpful review of the manuscript.

## References cited

Benna, P., Bruno, E., and Facchinelli, A. (1981) X-ray determination and equilibrium composition of clinopyroxenes in the system CaO-MgO-$Al_2O_3$-$SiO_2$. Contributions to Mineralogy and Petrology, 78, 272–278.

Biggar, G.M. (1985) Calcium-poor pyroxenes: Phase relations in the system CaO-MgO-$Al_2O_3$-$SiO_2$. Mineralogical Magazine, 49, 49–58.

Carlson, W.D. (1986a) Vanadium pentoxide as a high-temperature solvent for phase equilibrium studies in CaO-MgO-$Al_2O_3$-$SiO_2$. Contributions to Mineralogy and Petrology, 92, 89–92.

——— (1986b) Reversed pyroxene phase equilibria in CaO-MgO-$SiO_2$ from 925° to 1175°C at one atmosphere pressure. Contributions to Mineralogy and Petrology, 92, 218–224.

——— (1988) Subsolidus phase equilibria on the forsterite-saturated join $Mg_2Si_2O_6$-$CaMgSi_2O_6$. American Mineralogist, 73, 232–241.

Carlson, W.D., and Lindsley, D.H. (1988) Thermochemistry of pyroxenes on the join $Mg_2Si_2O_6$-$CaMgSi_2O_6$. American Mineralogist, 73, 242–252.

Gasparik, T. (1984) Two-pyroxene thermobarometry with new experimental data in the system CaO-MgO-$Al_2O_3$-$SiO_2$. Contributions to Mineralogy and Petrology, 87, 87–97.

Herzberg, C.T. (1978) Pyroxene thermometry and barometry: Experimental and thermodynamic evaluation of some subsolidus phase relations involving pyroxenes in the system CaO-MgO-$Al_2O_3$-$SiO_2$. Geochimica et Cosmochimica Acta, 42, 945–957.

Marfunin, A.S. (1979) Physics of minerals and inorganic materials, 340 p. Springer-Verlag, Berlin.

Mori, T., and Biggar, G.M. (1981) The composition of the liquid in the assemblage L + Fo + $Di_{ss}$ + $En_{ss}$ + Pl in the system CaO-MgO-$Al_2O_3$-$SiO_2$ at atmospheric pressure. In C.E. Ford, Ed., Progress in experimental petrology, D18, 144–147. Natural Environment Research Council Publications, London.

Obata, M. (1976) The solubility of $Al_2O_3$ in orthopyroxenes in spinel and plagioclase peridotites and spinel pyroxenite. American Mineralogist, 68, 355–364.

Perkins, D., III, and Newton, R.C. (1980) The compositions of coexisting pyroxenes and garnet in the system CaO-MgO-$Al_2O_3$-$SiO_2$ at 900°–1100°C and high pressures. Contributions to Mineralogy and Petrology, 75, 291–300.

Sen, G. (1985) Experimental determination of pyroxene compositions in the system CaO-MgO-$Al_2O_3$-$SiO_2$ at 900–1200 °C and 10–15 kbar using PbO and $H_2O$ fluxes. American Mineralogist, 70, 678–695.

Manuscript received August 29, 1988
Manuscript accepted November 25, 1988